LOW SPEED TESTING AND ANALYSIS

Fred Hermanspann

Presented at the XXV OSTIV Congress in St. Auban, France

Abstract

A flight test series was conducted to establish the low speed performance of a typical sailplane. The results are analyzed using a parametric drag build-up of the non-dimensional data. Dynamic effects due to speed decrease on minimum speeds are correlated with delays in stall related effects of the upper wing boundary layer. The same effects also apply to the associated additional drag terms near stall. Parametric drag build-up allows better definition of low speed performance from sparse test data and facilitates performance calculations.

Introduction

Flight performance at speeds below best glide ratio is of special interest for sailplanes (thermaling, etc.) and generally for all low power light airplanes (take off and landing, best climb, minimum power requirements, maximum altitude, etc.). At the same time establishment of flight performance from flight testing is becoming more difficult at low speeds because stall related effects make flight characteristics more nonlinear and increase flight test data scatter. A flight test and analysis study was made to understand the underlying flow field effects on lift and drag characteristics and to improve the data presentation. This included dynamic effects (from airplane deceleration) when approaching stall.

Discussion

Test Set-Up

The flight test program used the Chinook S - a homebuilt two-seat sailplane as a representative test configuration, see Figure 1. This sailplane has a wing with the 17 pct Wortmann FX67-K-170 airfoil (Reference A and B) and an aspect ratio of 22.6. It is built in mixed composite/aluminum construction and has an empty weight of 620 pounds. The airspeed is based on a nose pitot for total pressure and four static pressure ports halfway between wing and tail.

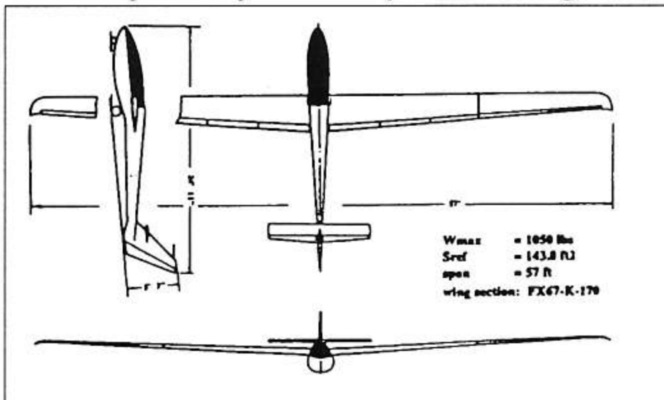

Fig. 1 Chinook S Sailplane

Video recording of the calibrated cockpit instrumentation was used as a low cost and versatile method to record data as well as data quality. In addition to recording standard flight data (specifically airspeed, altitude and air temperature) it also recorded bank angle, weather, sound and pilot comments. This allowed detailed post flight data screening to sort out usable data. It also provided time traces of air speed - important for the analysis of stall tests.

Minimum Speed Determination

Determination of the minimum speed of an airplane is important for safe flight operation and for comparisons of different configurations. It is very sensitive to the flight maneuver and has to be based on a consistent definition. The standardized stall maneuver consists of steady deceleration in straight flight until the g break where the airplane stalls - and the subsequent recovery, where lift is first lower and then higher than weight, see Figure 2. Provided that there is no roll-off before the g break and that the stall is not prevented by the elevator reaching the back stop, the g break is representative of the maximum lift capability of the airplane and is used here to define the minimum airspeed V_{min}. This minimum speed is somewhat higher (thus more conservative) than the stall speed, which is the minimum speed reached after the stall break but which is based on lift being smaller than weight.

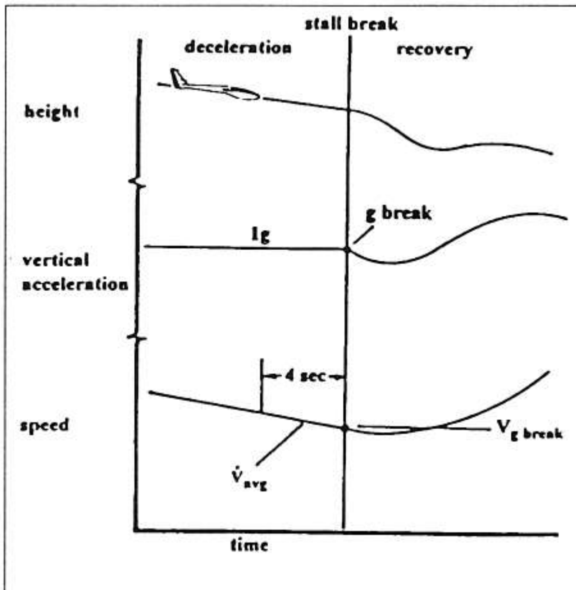

Fig. 2 Stall Maneuver

Note that the airplane reaches its minimum airspeed after the g break which is used to define the traditional stall speed. However, as lift is not equal to weight, this stall speed does not represent the maximum lift capability. Maximum lift is limited by flow separation on the upper wing surface as the angle of attack increases, the boundary layer is progressively thickened and weakened by the buildup of a leading edge suction peak and a subsequent steep pressure recovery. This causes the forward movement of first the boundary layer transition (on laminar flow airfoils) and then the separation point. The deceleration of airspeed when approaching stall - the stall entry rate - has a powerful effect in delaying these stall related effects. There is a time delay (or a phase lag) between the buildup of the upper surface suction peak and the above described stall related flow field changes resulting in a reduction of the minimum airspeed. This can be seen in Figure 3 where the minimum speeds of the Chinook S at various flap settings were plotted as function of stall entry rates.

W/S = 7.03 psf

V_g break measured after deceleration with V

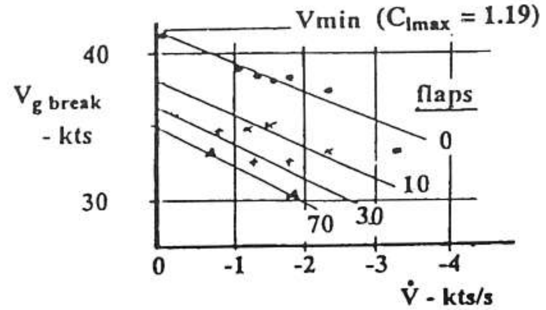

Fig. 3 Minimum Speed Determination

The apparent increase in maximum lift capability - the dynamic overshoot - seems to be proportional to the stall entry rate and comparison of different configurations can be easily masked by inconsistent entry rates. For example on the Chinook S a stall entry rate of-2 kts/s is equivalent to 10 degrees of flap deflection - indicating the importance of controlled stall tests. As deceleration rates at touch down can reach several knots per second this effect can lower touch down speeds significantly over low deceleration landings. As the dynamic overshoot for the maximum lift is tied to the time delay between buildup of the leading edge suction peak and the subsequent boundary layer separation on the upper wing surface, it should correlate with the characteristic time interval c/V - i. e. increasing effects for low speeds (V) or large chord lengths (c). Therefore one can expect increasing dynamic overshoot effects for low wing loading configurations such as ultralights, HPAs, solar powered airplanes, Martian flying platforms, birds, etc.. While a stall entry rate of - I kts/s is the established certification value, the definition of minimum speed (and thus the maximum lift coefficient CL_{max}) used in this study is based on zero deceleration (i. e. steady state).

Sink Rate Testing

Sink rates at various speeds were measured by standard timed descents at constant speed (compare references c and d). The results, corrected to standard sea level conditions and plotted in Figure 4, show considerable data scatter increasing towards the minimum speed. The faired speed polar indicates a best glide ratio of over 40 and a minimum sink rate of 117 fpm. Curve fitting these data points is somewhat arbitrary and a special effort was made to use underlying knowledge about the configuration drag buildup and the basic airfoil characteristics to define the speed polar, especially at the low speed end.

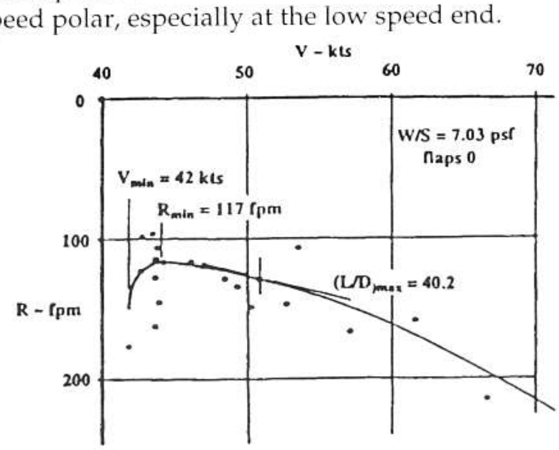

Fig. 4 Speed Polar - Chinook S

Drag Polar

In order to understand the drag buildup the speed and sink rate data were converted into nondimensional lift and drag coefficients. This allows analyzing the data in the time honored squared lift polar, see Figure 5.

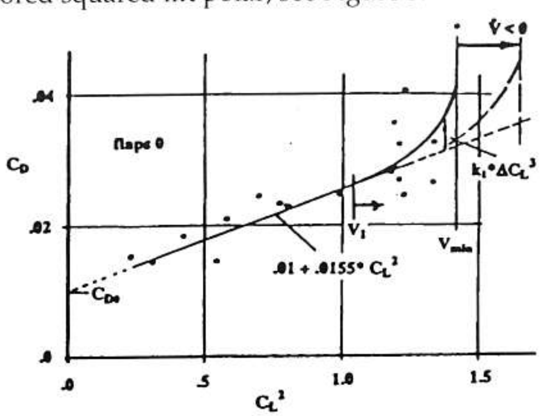

Fig. 5 Squared Lift Polar

In the main range of the lift coefficients the drag data behave linearly and allow a linear curve fit. This linear behavior corresponds to well attached flow and boundary layer transition points on all surfaces that move only slowly if at all. In this linear region drag can then be described as the sum of lift independent drag and a lift dependent drag term.

The lift independent term C_{DO} reflects mostly skin friction for a sailplane in clean configuration but can also include pressure drag for engine pods, landing gear or spoilers. The lift dependent term $k_o*C_L^2$ consists mostly of induced drag, but also includes drag changes due to changes in Reynolds number, lift coefficient, trim, and fuselage alignment. Therefore the correlation factor k_o is significantly larger than the induced drag factor $1/(\pi*AR)$ for ideal induced drag.

At high lift coefficients, when approaching stall the same stall related boundary layer effects that limit the maximum lift capability cause also additional drag. The forward movement of the upper wing transition and separation points increase upper surface skin friction and eventually cause substantial pressure drag. The available data points are insufficient to define this drag term accurately and other data sources were therefore used. The two-dimensional data from Reference A for the Chinook S wing section and three-dimensional results from Reference E, F and G were used in Figure 6 to define the additional drag term at high lift coefficients.

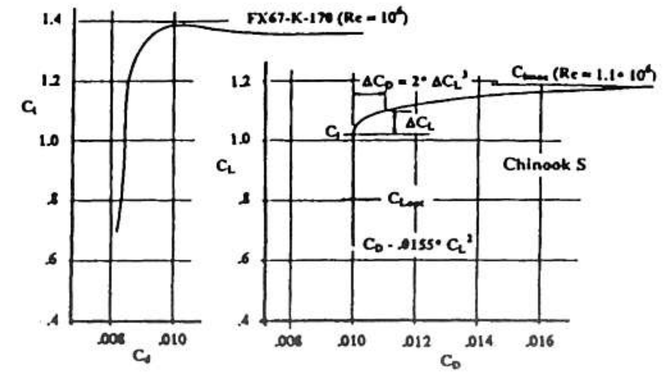

This additional drag can be described as

$\Delta C_D = k_1 * (C_L - C_{L1})^3$ with

C_{L1} onset of stall related

effects (C_{Lmax} - .17)

k_1 determined from

$\Delta C_D = C_{D0}$ at C_{Lmax}

The above formula is not based on established physical laws but it describes measured wind tunnel behavior and observed flow mechanisms, i. e. gradually increasing drag above the linear drag characteristics when approaching stall. Flight test data are usually less adequate to define these effects as described before. This drag buildup yields now a polynomial description of the drag polar that identifies the different drag contributions; allows non-dimensional comparison of different configurations and facilitates generation of performance data.

It stands to reason that if the same stall related effects, that determine maximum lift capability cause this additional drag term, then the same dynamic overshoot applies to drag. Therefore decelerating flight will delay this additional drag term to higher lift coefficients and improve the performance over steady state performance. This effect, indicated in Figure 5, will have a beneficial effect on stretching out landing flares (such as for International Birdman Rallye gliders) but may also result in too optimistic data from decelerating flight test near stall (compare Reference h).

It can be assumed that at low lift coefficients a similar effect occurs when the lower wing leading edge experiences a suction peak buildup and the lower boundary layer transition moves forward. However, there were no flight test data for the Chinook S was available to define such an additional drag term.

Low Speed Polar

Calculation of sink rates from this polynomial drag polar yields a smooth, numerically defined and physically plausible speed polar, see Figure 7.

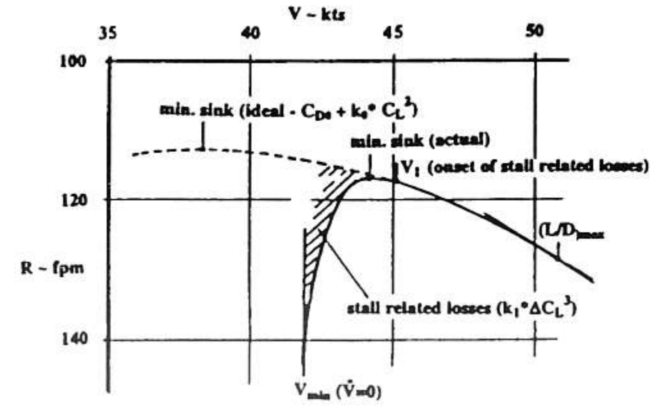

Fig. 7 Low Speed Polar

The minimum sink rate is now mathematically defined (117 fpm at 44.4 kts). It is interesting to compare this sink rate with the ideal minimum sink rate if there were no stall related effects on lift or drag, no detrimental upper surface boundary layer effects or no maximum lift limit. The minimum sink would only marginally be lower (113 fpm) but it would occur now at a significantly lower speed (38.6 kts). This ideal polar can be regarded as the upper performance boundary of this configuration with increased wing camber or flaps. Ideal flaps - increasing maximum lift without increasing drag level would be able to realize this potential. In real life full span, well sealed flaps come close to this ideal only at low flap deflections. Flight testing (such as Reference D) of modern sailplanes confirms that flap deflections generally do not reduce minimum sink, they only result in modest reductions of the speed for minimum sink. This illustrates that the numerical drag buildup by contribution is a useful method for the understanding and the calculation of sailplane performance.

Conclusions

Minimum speeds are very sensitive to stall entry rates and should be established with carefully controlled and documented stall maneuvers if used for comparison purposes.

Stall related effects - primarily the forward movement of boundary layer transition and separation on the upper wing surface - cause non-linearities in lift (determining minimum speeds) and additional drag terms (determining minimum sink).

These stall related effects are subject to dynamic overshoot - a shift to higher lift coefficients proportional to the stall entry rate.

Dynamic overshoot improves the low speed performance momentarily similar to deflection of ideal camber changing flaps.

The drag buildup from a lift independent term (mostly skin friction), a lift dependent term in the linear region (mostly induced drag and Reynolds number effects) and an additional term at high lift (stall related effects) is a functional and practical way to describe low speed drag of sailplanes and similar configurations.

This method helps one's understanding of drag contributions, allows correlation of 2D and 3D data, and provides a convenient, physically plausible determination of the speed polar from limited data.

This parametric drag characterization also facilitates performance calculations and comparisons of different configurations.

References

(A) D. Althaus, "Stuttgarter Profilkatalog," 1981.

(B) Fred Hermanspann, "Rain Effects on Laminar Flow Airfoils," AIAA 96-0899, 1996.

(C) Paul F. Bikle, "Polars of Eight," Soaring, June 1971.

(D) Richard H. Johnson, "The Johnson Flight Tests," 1980.

(E) L. M. M. Boermans, D. C. Terleth, "Wind Tunnel Tests of Eight Sailplane Wing-Fuselage Combinations," OSTIV 1983.

(F) Fred Thomas, "Basics for the Design of Sailplanes," 1990.

(G) Z. Gabrijel et al, "Wind Tunnel Experiments on the Model of Yugoslav World Class Glider," Technical Soaring, Oct. 98.

(H) "On the Identification of the Speed Polar during Normal Soaring Flight", Technical Soaring Apr. 94.